PUBLIK ENGINEER

Journal of Engineering for **Rookies**

Pseudo-homogeneous CSTR Simulation of a Fluidized Bed Reactor operating in condensed-mode including Sanchez-Lacombe n-hexane co-solubility effect predictions

P. Rainho[a], A. Alizadeh[b], M. R. Ribeiro[c], Timothy. F. L. Mckenna[b]

[a] *Chemical Engineering department, Instituto Superior Técnico – Universidade de Lisboa, Av. Rovisco Pais, 1049-001 Lisbon, Portugal*

[b] *C2P2 - LCPP Group, UMR 5265 CNRS, Université deLyon, ESCPE Lyon, Bat 308F, 43 Bd du 11 novembre1918, F-69616, Villeurbanne, France*

[c] *Institute for Biotechnology and Bioengineering (IBB), Instituto Superior Técnico – Universidade de Lisboa, Av. Rovisco Pais, 1049-001 Lisbon, Portugal*

Received 30 September 2014; received in revised form 23 October 2014; accepted 10 December 2014

Abstract

This work explores the impact of the **inert condensing agent** (ICA) **n-hexane** in the production of **Polyethylene** via gas-phase **condensed mode** bed reactor. The gas loaded to these reactors contains mainly ethylene, nitrogen and other reaction agents like hydrogen. But it also includes condensed inert agents like n-hexane. They have an important role in **cooling down** the bed of the reactor not only because they have a relevant heat capacity but primarily because they can be in a condensed state. As the gas-liquid mixture enters the reactor, the condensed liquid content vaporizes and removes latent heat that way allowing bigger productions. ICA's like hexane seem, in addition, to **solubilize** the **ethylene** gas in the **amorphous polyethylene** of the **growing polymer phase** (co-solubility effect) enabling even higher polymerization rates. The **Sanchez-Lacombe** equation of state have been successfully used in predicting the mentioned co-solubility effect of n-hexane in ethylene polymerization. Its lately computational predictions on such subject were used in the current work. This work simulates a reacting system composed by an **ethylene/nitrogen/n-hexane gas phase** in equilibrium with an **ethylene/amorphous polyethylene/n-hexane polymer phase**, using a pseudo-homogeneous steady-state CSTR approach. This system was evaluated at **7 bar** ethylene, **1 bar** nitrogen and within a range of **0.0 - 1.0 bar n-hexane**, with different operation conditions such as **catalyst flowrates**, **inlet gas temperature** and **kinetic rate constants**.

The global results showed that from **no hexane** in reactor to a pressure of **0.1bar** hexane there's a variation of polyethylene production of about **2%** (**n-hexane co-solubility effect**). And as total pressure adds **0.1bar** hexane, the polyethylene production variation approximately follows this trend; it is like this as far as **inlet stream cooling capacity** is not too high (declining temperature and, by extension, kinetics) that it subordinates the n-hexane co-solubility effect. Regarding reactor temperature, there are two distinct behaviours: if the reactor operates in a non-condensed mode (less than **0.4bar** hexane), there's a moderate decrease of temperature (**2%** maximum) with rising hexane pressure. It falls down much faster when the reactor starts to operate in a condensed-mode reaching the **8%** variation for each 0.1bar hexane increasing step.

Keywords: Condensed-mode; inert condensing agent; n-hexane; gas-phase ethylene polymerization; Sanchez-Lacombe; FBR with pseudo-homogeneous CSTR approach

1. Introduction

As it is well known, the PE is the most produced and best known polymer in the world. The enormous global market of polyolefins and the projection about future demand for these materials is reason enough for the leaders in this field to invest on research and development. The polymerization of ethylene on supported catalyst in gas phase fluidized bed reactors (FBR's) continues to be the predominant process for production of Linear Low Density PE (LLDPE). A critical issue in this process is the heat removal resultant from polymerization, making the rate of polymer production to be significantly limited. One way of increasing the heat removal is to use a condensed mode cooling operation (CMO). The gas fed to the FBR contains, besides ethylene and other reaction agent gases, a mixture of inert condensing n-alkanes gases. When they enter the reactor, they almost immediately vaporize removing heat this way. Now in the gas phase, they are able to diffuse into polymer particles like ethylene. Initially, ethylene gets in touch with young catalyst particles, it diffuses into their pores and it starts to polymerize. By this time, catalyst particle fragments into smaller fragments. As the reaction proceeds, the ethylene has to start sorbing into the polymer phase in order it can achieve the active sites. As

the polymer layer covering the active sites is essentially made of amorphous polyethylene, the rate of reaction will be determined by the concentration of ethylene in the amorphous phase of PE. This concentration of ethylene in the amorphous phase seems to be enhanced by an inert specie like n-alkanes. To describe and simulate this suggestion it's necessary to understand how the n-alkane is providing this more accessibility of ethylene in reaction centers. Thermodynamic models like Sanchez-Lacombe have given strong answers on it. This local/micro-scale phenomena increases kinetics that, in turn, will lead to bigger reactor productions. That's what it will be confirmed in this study with ICA n-hexane.

2. Science and engineering needed

As already mentioned, the feed stream of polyethylene in a FBR is a mixture of different components with different functionalities. So for more realistic modelling it should be included at least **ternary phase** in polymer solubility species studies. Some thermodynamics models have been tested to predict and account ethylene solubilization. The **Sanchez-Lacombe** (SL) equation of state (EOS) [1] is one of the most applied models in simulation of polymer phase thermodynamics [2]. In this work it will be used its most lately results concerning ethylene solubility and concentration in growing polymer phase when it's present n-hexane. Several studies for LLDPE production have included **particle growth models** that led to a better understanding of the reactor behavior as well as properties of the polymer produced. Modelling at the particle level requires not only thermodynamics but naturally transfer phenomena too. Nevertheless it has been established in the literature that, under many conditions, heat transfer and diffusional resistances do not play an important role at the particle level in gas-phase polyethylene reactors when it is already in a mature/developed state [3]. Under this statement, and since it meets the purposes of this work, it will be considered only thermodynamics. Deeper considerations are in topic 2.1.

Modelling fluidized-bed polymerization reactors is not simple since many interactions between phases need to be taken into account. The fluidized reactor model mostly accepted relies on **Kunni & Levenspiel fluidized bed theory** [4]. In their model, the gas flows up the reactor in the form of **bubbles** exchanging gas with reactive particles (like catalysts) in a called **emulsion** phase. The product formed in these particle then returns back into a bubble and leaves the bed when it reaches the top of the reactor. The fluidized bed reactors for LLDPE production have been modelled as single, two, or three-phase reactors. In topic 2.2 will be discussed the **single-phase modelling** once it's the similar approach mode used in this work, despite the simple pseudo-homogeneous steady-state CSTR admitted here has no mass and heat transfer concerns nor even accurate FBR's description as well.

2.1. Sanchez-Lacombe n-hexane co-solubility effect prediction

The rate law of ethylene polymerization adopted in this thesis is the one proposed by Floyd [5]. It's a simple catalytic **single-site** and **first order rate** with respect to the ethylene concentration at the active sites of catalyst. Formally, the local rate of polymerization inside a polymer particle can be expressed as:

$$R_{p,loc.} = k_p C^* C^*_m \qquad \textbf{(1)}$$

$R_{p.loc}$ – local ethylene polymerization rate
k_p – kinetic constant rate
C^* – local concentration of active sites in a catalyst fragment
$C^*_{et.}$ – ethylene local concentration in the polymer phase surrounding some catalyst fragment

To predict satisfactorily the ethylene concentration in amorphous polymer phase, C^*_m in eq. 1, a thermodynamic model has to be capable of detecting the effect of n-hexane on the ethylene solubility and polymer swelling. The figure 1 illustrates a polymer particle in a ternary system. The particle surrounded by a gas phase (a) is zoomed until a catalyst fragment surrounded by produced semi-crystalline polyethylene (b) which in turn is zoomed until a mix of polymer chains are viewed to be immobilized on the surface of catalyst fragment (c). Both ethylene (red) and n-hexane (in blue) are present.

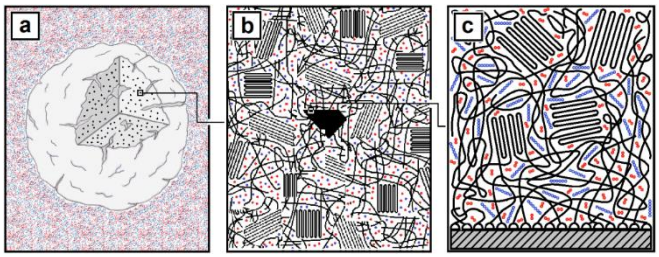

Figure 1 – Schematic representation of ethylene-n-hexane-polyethylene ternary system at different scale levels. (Alizadeh A. , 2014, Figure 4.3)

Hutchinson and Ray [6] have developed thermodynamic models to predict equilibrium monomer concentrations at the catalyst sites from external gas-phase monomer concentrations in the vicinity of the polymer particles. Kosek [3] explored the advantage of the steady-state modeling as the possibility of dependence of temperature and concentrations in the particle on model parameters. He found that for many catalyst systems in which heat and mass transfer resistances do not influence monomer concentrations and temperatures within the polymer particles, the monomer concentration at the catalyst sites is determined by the equilibrium sorption of the monomer within the polymer particles.

Yang [7] measured the solubility of ethylene/isopentane and ethylene/n-hexane in semicrystalline PE of crystallinity of 48.6%, at temperatures of 70, 80, and 90°C, 2 MPa total pressure, 80–190KPa isopentane pressure and 20–90KPa n-hexane pressure. He concluded isopentane and n-hexane increase the solubility of ethylene in the corresponding ternary system. On the contrary, the solubility of isopentane or n-hexane remains unchanged with an increase of the ethylene partial pressure.

Bashir et al. [8] used SL EOS predictions in the multicomponent system of ethylene/1-hexene/LLDPE-1-hexene mixture at 70°C, 90°C and 150°C. Their predictions were in good agreement with the experimental data. They also noted the solubility enhancement is co-monomer-type dependent.

Alizadeh [9] extended the application of Sanchez-Lacombe EOS from the binary system of ethylene/PE to the ternary system of ethylene/n-hexane/PE in order to describe the change in concentration of ethylene in the amorphous phase of polyethylene. He fitted his SL predictions with the sorption equilibrium data acquired by group of Yang [7] by adjusting the binary interaction parameters (k_{ij}). Yang's team used some commercial LLDPE at three equilibrium temperature of 70, 80, and 90 °C, up to 20 bar total pressure and up to 1 bar n-hexane. In a global conclusion, the trend predictions of ternary SL model area according to Yang's group experimental data but they have outputted some overestimation of the solubility of both ethylene and n-hexane (except for ethylene solubility at 90 °C and 5bar total pressure). But as the equilibrium temperature increases, the predicted solubility magnitude overestimation for both ethylene and n-hexane is decreased.

2.2. Gas-phase ethylene polymerization in a FBR and condensed-mode operation

The polymerization of ethylene on supported catalyst in gas phase FBR's is the most common process for production of LLDPE. A small amount of high activity catalyst particles, with diameter of 10–50μm, is supplied continuously or semi-continuously to the reactor carried by nitrogen. Before they enter the reactor, they can be pre-activated and/or prepolymerized. Catalyst injection rates are in the range of 0.001-0.05 g/s depending on catalyst activity and reactor capacity. Since the catalyst particles are the smallest/less dense in the reactor they move upwards. But at the same time they are moving upward, they are increasing their size due to the polymerization. The gas feed should be designed in order to not elutriate the particles having in account their maximum weight (which depends on their residence time). As these catalyst particles are exposed to monomer or monomer mixture in the reactor, polymerization occurs almost immediately and the catalyst particles are quickly encapsulated by the newly-formed polymers to a size of around 300–1000μm. Their sizes (naturally depending on their residence time in the reactor) range from the initial catalyst particle diameter to the large particle in the bed, composed by that time mostly of polymer. In the first stage of particle life, the polymer starts to fill the pores of the supported catalyst particle and a gradual fragmentation of the catalyst support takes place. However, the fragments are kept together by the polymer. The time-scale of the fragmentation process ranges from fractions of a second to a few seconds. The reaction heat is dissipated from the growing polymer particles by a fast growing gas stream. Fully-grown polymer particles are withdrawn continuously or intermittently from the bottom portion of the reactor (above distributor plate) while keeping the bed level approximately constant. The superficial gas velocity can vary from 3 to 8 times the minimum fluidization velocity [10]. Since very high fluidizing gas velocity is used for heat removal purpose, the monomer conversion per pass is quite low (<5%) and a large amount of unreacted gas containing an inert gas leaving the reactor is cooled, compressed, and recycled back to the reactor. An inert hydrocarbon liquid may also be added to the recycle gas stream to increase the reactor heat removal capacity (condensed mode operation) and hence to increase the polymer throughput. Overall conversion is about 98% [11]. Industrial fluidized bed reactors typically operate at temperatures of 75-110°C and pressures of 20-40 bar [12]. The pressure drop across the bed is slightly higher than the weight of the particles divided by the cross sectional area.

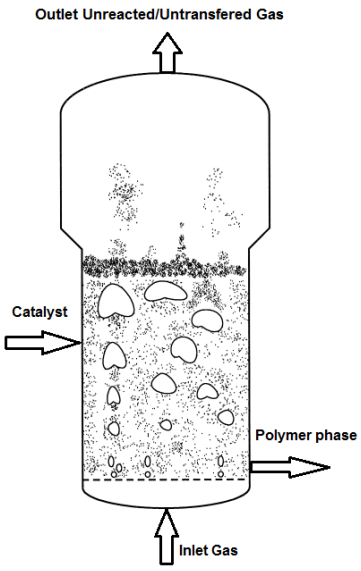

Figure 2 – Gas-phase FBR illustration for ethylene polymerization

In case of low to moderate activity of the catalyst, heat transfer and diffusion resistances do not play an important role at the particle level in the gas-phase polyethylene reactors. In the limiting case, where either bubbles are small or interphase mass and energy transfer rates are high and catalyst is at low to moderate activity, intraparticle temperature and concentration gradients are negligible [5]. In this case, LLDPE production fluidized bed reactors could be modelled as a CSTR proposed by McAuley et al. [11], [12]**.** He considered the polymerization reactor to be a well-mixed one. For this to be a well-mixed reactor, the **mixing index** (particles degree of mixing in the reactor) should be near by 1 [13]. McAuley et al. revised Choi and Ray's model [14]. In both works, the emulsion phase is assumed to behave as a CSTR fully mixed. This assumption is good for small fluidized-beds that are violently fluidized and have a height to diameter ratio close to one, as it was demonstrated by Lynch and Wanke [15]. However for a typical ethylene polymerization reactor, mixing index is about 0.4-0.5. This indicates a low reactor mixing and makes a single CSTR a not very realistic approach. Alizadeh et. al. [16] employed a tanks-in-series model to represent a pseudo-homogeneous model for predicting the performance of an industrial-scale gas-phase polyethylene production reactor. Weijuan et al. [17] simulated the steady-state behavior of industrial slurry polymerization of ethylene in 2 continuous stirred tank reactors. The model demonstrated that changing the catalyst flow rate, changes simultaneously the mean residence-time in both reactors, which plays a significant role on the establishment of polyethylene architecture properties such as molecular mass and polydispersity index.

The **condensed mode operation** in the gas-phase fluidized bed ethylene polymerization process increases the space-time yield of polymer production. The cooling capacity of the recycle gas stream is increased by addition of non-polymerizing condensable agents in order to increase the dew-point temperature of the stream. An even further increasing in cooling capacity is achieved in the super-condensed mode operation [18]. This is actually a mean of expanding the plant capacity without resizing the reactor. Ramanathan [19] used a CSTR with a polymer phase very well-mixed and a residence-time for polymer particle of several hours. The catalyst was present in the polymer phase and the solubility of monomers and other reactants were predicted by SL. In his simulation with 3 different catalysts he concluded that the polymer produced, cooler duty and the

amount of condensation in recycle stream are the same for dry or wet mode. There is about 160 % increase in productivity if 10 mole % of liquid is present in the recycle stream. Mirzaei [20] used Peng-Robson EOS for flash calculations to evaluate the liquid fraction as well as the gas and liquid composition in the inlet stream to the reactor. For polymer particles, he used SL EOS in order to calculate the concentration of monomers, hydrogen and condensable components from the concentration of the components in the gas phase. Their results were according to some patent they used for comparison.

Alizadeh and Mckenna [21] thought the liquid to evaporate at hot spots in the bed. Parameters like droplet size, size distribution, heat of vaporisation and properties of solid particle phase as well as eventual contact between these two phases will control the overall vaporisation process of the liquid droplet in the presence of fluidising solid particles. They analysed time scales for droplet heat up and vaporisation compared in case of homogenous vaporisation of the droplet. Based on their assumptions and calculations they expected the major part of the liquid injected through the bottom of an FBR to vaporise at a height of between 1 and 2m. Since the evaporation process is quite rapid, the gas phase will be quite rich in the heavier ICA and so the polymer.

3. Reactor model

The reactor model developed in this work consists in a **pseudo-homogeneous CSTR** type. It's assumed that all bed operates in such approach. There are no concerns about mass or heat transfer phenomena nor real fluidizing bed reactor characteristics. Based on this, it will be assumed a simple model in steady-state that can give important indications on how the **reactor temperature** and **polyethylene mass rate** vary with different **hexane pressures** and for different sets of conditions such as different **kinetic constants**, $\mathbf{k_p}$, **catalyst flowrates,** $\mathbf{Q_{c.0}}$, and **inflow temperatures,** $\mathbf{T_0}$.

First, all the assumptions for this reactor simulation will be enumerated. Then the model equations are written and briefly commented. Finally the results of simulations are shown in plots and discussed. In the end it's made a sensible analysis to some parameters of balance equations to check which are the ones that may strongly twist the results.

3.1. Assumptions

- ✓ Single-phase CSTR approach
- ✓ 1 inlet flow containing a mixture of **ethylene**, **n-hexane** and **nitrogen**
- ✓ 1 inlet solid flow containing the catalyst
- ✓ 1 outlet gas flow containing ethylene, n-alkane and all nitrogen
- ✓ 1 outlet solid flow containing the **polymer phase** which includes **catalyst**, **polyethylene**, **dissolved ethylene** and **n-hexane**. Dissolved nitrogen in the particle is negligible and it's considered to be zero.
- ✓ Equilibrium is **instantaneous** and particles are mature (no mass or heat transfer phenomena in every volume of reactor and particles)
- ✓ The **absorbing latent heat species** (n-hexane and ethylene) do it **instantaneously**
- ✓ Elutriation of solids is neglected at the top of the bed
- ✓ No pressure gradient or even difference pressure between reactor inlet and outlet
- ✓ The catalyst particle size is spherical shape and **mono-dispersed**
- ✓ Fast catalyst activation
- ✓ Spherical and Constant mean particle size

The reacting volume is the catalyst volume, V_c. There's an inflow of catalyst and an inflow of gas of ethylene, n-hexane and nitrogen. The outflows are composed by the polymer phase and the gas not reacted and not dissolved as well in polymer phase. The reactor is also characterized by a bed height, h_b, and a base area, b.

3.2. Model Equations

The model equations consist essentially in a steady-state **polyethylene mass balance** and a **global heat balance** in a CSTR approach. They are exposed in the next lines as well as the terms constituting them.

- ***Polyethylene Mass Balance (PEMB)***

The polyethylene production, $m_{Pet.}$, is evaluated in mass balance according to:

$$R_p(T,P)V_c - \dot{m}_{Pet} = 0 \qquad \textbf{(2)}$$

The reaction rate, R_p, is an extrapolation of eq.1 for every particle in the reactor. It's an average polymerization rate.

$$R_p(T,P) = k_p(T)C^*C_{et.}^p(P)M_{et} \qquad \textbf{(3)}$$

The concentration of ethylene in polymer phase, $C_{et.}^p$, is a function of hexane pressure. Its variation was predicted in Alizadeh work [9] with SL EOS and such data is in table 2.

The kinetic constant, k_p, has an Arrhenius temperature dependence:

$$k_p(T) = k_p^{T_{\exp.}} e^{\frac{E_a}{R}\left(\frac{1}{T_{\exp.}} - \frac{1}{T}\right)} \qquad \textbf{(4)}$$

The catalyst active concentration, C^*, is obtained through a mass balance to the active moles of catalyst in the reactor:

$$Q_{c.0}C_0^* - Q_cC^* - k_d(T)C^*V_c = 0 \qquad \textbf{(5)}$$

Solving for C^* and with catalyst outflow, Q_c, equal to catalyst inflow, $Q_{c.0}$:

$$C^* = \frac{C_0^*}{1 + k_d(T)\frac{V_c}{Q_{c.0}}} \qquad \textbf{(6)}$$

The deactivation constant, k_d, has also an Arrhenius temperature dependence:

$$k_d(T) = k_d^{T_{exp.}} \cdot e^{\frac{E_d}{R}\left(\frac{1}{T_{exp.}} - \frac{1}{T}\right)} \quad \textbf{(7)}$$

- ***Heat Balance (HB)***

$$\Delta H_r^T \dot{m}_{Pet} - (T - T_0)\left[\dot{m}_g \bar{c}_{p.g} + \dot{m}_p \bar{c}_{p.p}\right] - F_0{}^L \Delta H_v^{T_0} = 0 \quad \textbf{(8)}$$

Left eq. 8 term respects to the polymerization heat, middle one represents sensible heat and right one denotes global heat vaporization term. This one, $F_0{}^L\Delta H_v$, is the weighted sum of n-hexane and ethylene vaporization rate contributions:

$$F_0{}^L \Delta H_v^{T_0} = \left(F_{hex.0}{}^L \Delta H_{v.hex.}^{T_0} + F_{et.0}{}^L \Delta H_{v.et.}^{T_0}\right) \quad \textbf{(9)}$$

The amount of liquid hexane ($F_{hex.0}{}^L$) and ethylene ($F_{et.0}{}^L$) in eq. 9 were estimated, for the work temperatures and pressures, with Redlich-Kwong-Soave (RKS) equation of state (in Aspen®). The inflow stream gas should enter the reactor in a liquid-gas equilibrium mixture. And once inside, it should vaporize totally (and instantaneously). To know what are the appropriate thermodynamic conditions for the inlet flows, so that their content can vaporize at the reactor pressure and temperature, it's necessary phase equilibria data. The numerical mass liquid fractions predicted for this work are shown in table 2.

The hexane vaporization heat is estimated by a Watson type correlation [22]. For ethylene vaporization heat it was used the ethylene thermodynamic EOS predictions of Smulaka [23] by fitting his results at 10bar pressure. Corresponding expressions are in eq. 10 and eq. 11 respectively.

$$\Delta H_{v.hex.} = 45.61\left(1 - \frac{T}{507.43}\right)^{0.401}, \quad 342 \le T(K) \le 480 \quad \textbf{(10)}$$

$$\Delta H_{v.et.}(10bar) = -0.0202T^2 - 72.836T + 112.72, \quad -98.15 \le T(K) \le -53.15 \quad \textbf{(11)}$$

A small caveat about ethylene presence in vaporization process and its vaporization heat correlation (eq.11) shall be said. Although **pure ethylene** is clearly a gas in working pressure conditions, it was included in vaporization phenomena simply because that's what RKS model predicted in the **binary scenario**. So, to maintain consistency, it was assumed to be also in gas-liquid equilibrium. RKS model estimates there is about a 10-15% liquid ethylene fraction in the range of work conditions. Thus it is a noticeable amount. Concerning ethylene heat vaporization correlation at 10bar total pressure (eq. 11), one notices it boils at -53.15°C. Using such eq. out of the temperature range is admitting a pseudo-liquid state for ethylene at higher temperatures. It may not be the most corrected consideration; but assumed the prediction of RKS model of an ethylene liquid state in the working conditions it makes necessary to have some estimation of it.

The outlet gas mass, m_g, in eq. 8 is the sum of the three existing gases:

$$\dot{m}_g = \dot{m}_{et.} + \dot{m}_{hex.} + \dot{m}_{N2} \quad \textbf{(12)}$$

And each of its terms are (through specie mass balance):

$$\dot{m}_{et.} = \dot{m}_{et.0} - \dot{m}_{et.d} - \dot{m}_{Pet.} \quad \textbf{(13)}$$

$$\dot{m}_{hex.} = \dot{m}_{hex.0} - \dot{m}_{hex.d} \quad \textbf{(14)}$$

$$\dot{m}_{N2} = \dot{m}_{N2.0} \quad \textbf{(15)}$$

With ethylene and hexane dissolved mass in polymer phase, $m_{et.d}$ and $m_{et.d}$ respectively, equal to:

$$\dot{m}_{et.d} = \frac{C_{et.}^p M_{et.}}{\rho_p} \dot{m}_{Pet.} \quad \textbf{(16)}$$

$$\dot{m}_{hex.d} = \frac{C_{hex.}^p M_{hex.}}{\rho_p} \dot{m}_{Pet.} \quad \textbf{(17)}$$

$M_{et.}$ and $M_{hex,}$ are ethylene and hexane molar masses.

In what concerns polymer mass term, m_p, in eq. 8 it is the sum of polyethylene mass rate, $m_{Pet.}$, catalyst mass rate, m_c, and ethylene plus hexane dissolved mass rate in polymer phase, $m_{et.d}$ and $m_{hex.d}$ respectively:

$$\dot{m}_p = \left(\dot{m}_{Pet.} + \dot{m}_c + \dot{m}_{et.d} + \dot{m}_{hex.d}\right) \quad \textbf{(18)}$$

With the proper algebra and substitutions, the final mass and heat balance system is:

$$\begin{cases} PEMB.: \dot{m}_{Pet} = k_p^T(T) C^* C_{et.}^p V_c \\ HB.: \dot{m}_{Pet} = \dfrac{F_0{}^L \Delta H_v^T + (T - T_0)\left[\dot{m}_{g.0} \bar{c}_{p.g} + \dot{m}_c \bar{c}_{p.p}\right]}{\Delta H_r^T - (T - T_0) f\left(\bar{c}_{p.p} - \bar{c}_{p.g}\right)} \end{cases} \quad \textbf{(19)}$$

With initial inlet gas mass rate, $m_{g.0}$:

$$\dot{m}_{g.0} = \dot{m}_{et.0} + \dot{m}_{hex.0} + \dot{m}_{N2.0} \quad \textbf{(20)}$$

The letter **f** in eq. 19 is abbreviating the following quantity:

$$f \equiv \left(1 + \frac{C_{et.}^p M_{et.}}{\rho_p} + \frac{C_{hex.}^p M_{hex.}}{\rho_p}\right) \approx 1 \quad \textbf{(21)}$$

To calculate the bed volume, V_b, polymer particle volume, V_p and catalyst volume, V_c, it was used:

$$V_b = b h_b = \pi 4^{-1} d^2 h_b \quad \textbf{(22)}$$

$$V_p = V_b(1 - \varepsilon) \quad \textbf{(23)}$$

$$V_c = n_c \frac{\pi}{6} d_c^3 = V_p\left(\frac{d_c}{d_p}\right)^3, n_c = n_p \quad \textbf{(24)}$$

The reactor base area, b, and bed height were fixed. With it, bed volume, V_b, is straightforward (eq. 22) as well as polymer particle volume, V_p, (eq. 23) at some typical fluidizing porosity, ε. The diameter and height of the fluidized bed reactor were adjusted to be in a usual range of industrial reactors. According some patents they are [10-15]m for bed height and [2.44-4.4]m for bed diameter [24]. In turn, the catalyst volume, V_c, needed for this particle volume was calculated assuming particles are **spherical shaped** and assuming each catalyst particle will turn into each polymer particle. So total number of polymer particles, $\mathbf{n_p}$, are equal to the total number of catalyst particles, $\mathbf{n_c}$.

$$V_p = n_p \frac{\pi}{6} d_p^3 <=> n_p = \frac{6}{\pi} V_p d_p^{-3} \quad \textbf{(25)}$$

The catalyst volume finally comes the eq. 24. The catalyst and particle diameter, d_c and d_p, were adjusted according reference values. They are [30-50]μm for catalyst particle and [300-1000]μm for polymer particle [12].

The volumetric inlet gas flowrate, $Q_{g.0}$, is useful to check the proper range of superficial gas velocity value:

$$Q_{g.0} = \frac{\dot{m}_{g.0}}{\rho_g} \quad \textbf{(26)}$$

With eq. 26 and the base area of reactor fixed, the superficial velocity of gas, $u_{g.0}$ is:

$$u_{g.0} = \frac{Q_{g.0}}{b} \quad \textbf{(27)}$$

According some patents [24], [25] these velocities are around $0.48<u_{g.0}<1$ m/s.

The average particle residence time, σ_p, is defined as the quotient between particle volume in the rector, V_p, and the volumetric inflow rate, Q_0, which comprises catalyst volumetric inlet rate, $Q_{c.0}$, and gas volumetric inlet rate that contributes to polymerization, $Q_{g.0}$'. Q_0 is numerically the same as the polymer volumetric outlet rate, Q_p.

$$\sigma = \frac{V_p}{Q_0} = \frac{V_p}{Q_{c.0} + Q_{g.0}'} = \frac{V_p}{Q_p} \quad \textbf{(28)}$$

The bulk density of the fluidized bed, ρ, is estimated by:

$$\rho = \frac{m_b}{V_b} = \frac{(1-\varepsilon) b h_b \rho_p + \varepsilon b h_b \rho_g}{b h_b} \quad \textbf{(29)}$$

m_b is the mass of the bed. Reducing eq. 29:

$$\rho = \rho_p + \varepsilon(\rho_g - \rho_p) \quad \textbf{(30)}$$

3.3. Data tables

The left side of table 1 contains the thermodynamic and catalyst parameters established by Alizadeh in his work [9]. They are used in the current simulation. The right side shows the parameters and numerical volumes concerning reactor.

Table 2 contains, in first left half, equilibrium data for the **concentration of ethylene** and **n-hexane** in **polymer phase**. The original data was extracted from Alizadeh work [9] and it consisted in 4 predictions of the mentioned concentrations at 4 hexane pressures – 0.2, 0.3, 0.6 and 0.8 bar. These values were interpolated in order to have a more continuous range of hexane pressures. The correlation obtained was also extrapolated for 0.9 and 1.0bar hexane. The 2nd right half of the table shows the **mass liquid fraction, $\mathbf{m_{liq.}}$**, of inlet stream at 40, 45 and 50°C, predicted by Redlich-Kwong-Soave (RKS) equation of state. It is also indicated the dew-point at given conditions. Below 0.40 bar n-hexane (including) there's no liquid phase (dew-point is below the inlet flow temperature). On the other hand, the maximum percentage of liquid mass in the flow is at 1bar hexane. At 40°C inlet flow, there is no liquid until hexane pressure reaches 0.5bar. From this level until 1 bar hexane, the amount of liquid is always increasing. At 45°C, only at 0.60 bar hexane pressure starts to exist liquid in inlet flow. Finally the 50°C temperature flow only starts to have liquid at 0.70 bar hexane pressure. The liquid quantity fractions, at the same hexane pressure, decreases with increasing temperature.

Table 3 displays the **Simulation I** results. It fixes total molar flow, **F**, inlet temperature, $\mathbf{T_0}$, and catalyst flowrate, $\mathbf{Q_c}$, for 3 different values of referential $\mathbf{k_p}$. The simulation results table show polyethylene mass rate, $\mathbf{m_{Pet.}}$, reactor temperature, **T**, ethylene conversion, **%Conv.**, polymerization rate, $\mathbf{R_p}$, superficial gas velocity, $\mathbf{u_{g.0}}$, and average particle residence time, $\boldsymbol{\sigma_p}$. The $\mathbf{m_{Pet.}}$ and **T** are represented in plots in topic 3.4. Besides Simulation 1, there is Simulation 2 and Simulation 3. Their numerical output are omitted and they're only represented in plots (in terms of $\mathbf{m_{Pet.}}$ and **T**). Thereat, the characteristics of such simulations and discussions on their results are exposed

Table 1 - General parameters/constants used in simulations. General thermodynamic and catalyst parameters were extracted form Alizadeh work.

General thermodynamic parameters			**Reactor Parameters**	
$T_{exp.}$ (°C)	$P_{et.}$ (bar)	P_{N2} (bar)	d (m)	b (m^2)
80	7.00	1.00	4.0	12.6
$C_{p.c}$ ($J.kg^{-1}.K^{-1}$)	$(-\Delta H_r^{80°C})$ ($J/mol_{et.}$)	$C_{p.p}$ ($J.kg^{-1}.K^{-1}$)	h_b (m)	V_b (m^3)
2000	107 600	2000	10.7	134
Catalyst parameters			ε	d_p (μm)
$k_d^{80°C}$ (s^{-1})	E_d (kJ/mol)	E_a (kJ/mol)	0.55	500
$1.00x10^{-4}$	42	42	V_p (m^3)	d_c (μm)
ρ_c (kg/m^3)	C_0^* (mol/m^3_c)		60.4	30
2300	0.55		V_c (L)	
			13	

Table 2 - Working thermodynamic conditions relating to polymer phase ethylene concentration, polymer phase hexane concentration, liquid fraction of inlet flow at different inlet temperatures

			Inlet mass liquid fraction, $m_{liq.}$			
$P_{hex.}$ (bar)	$C_{et.}^{P}$ **(mol/m^3_p)**	$C_{hex.}^{P}$ **(mol/m^3_p)**	40°C	45°C	50°C	$T^{Dew\text{-}point}$ (°C)
0.00	84.29	0.00	-	-	-	-
0.10	86.03	38.17	-	-	-	-
0.20	87.96	79.20	-	-	-	-
0.30	90.07	123.08	-	-	-	-
0.40	92.37	169.82	0.00%	0.00%	0.00%	38.8
0.50	94.86	219.42	3.91%	0.00%	0.00%	43.6
0.60	97.53	271.86	8.66%	3.46%	0.00%	48.1
0.70	100.39	327.16	13.02%	8.04%	2.61%	52.3
0.80	103.44	385.32	17.03%	12.26%	7.06%	56.1
0.90	106.67	446.33	20.89%	16.27%	11.23%	59.7
1.00	110.08	510.20	24.17%	19.77%	14.97%	63.1

Table 3 - Simulation I results for 3 different reference propagation kinetic constant, $k_p^{80°C}$.

SIMULATION I Results						
Molar Gas flow rate, F (mol/s) **2000**		T_0 (°C) **40.0**		Catalyst flow rate (g/s) **0.222**		
	$k_p^{80°C}$ (m^3_{Pet}.mol-site^{-1}.s^{-1}) **1200**					
$P_{hex.}$ (bar)	**m_{Pet} (ton/h)**	**T (°C)**	**% Conv.**	**R_P ($kg_{Pet}.m_c^{-3}.h^{-1}$)**	**$u_{g.0}$ (m/s)**	**σ_p (h)**
0.00	5.295	107.8	2.62	405334	0.52	10.5
0.10	5.409	105.8	3.10	412928	0.53	10.2
0.20	5.502	103.8	3.19	422200	0.53	9.93
0.30	5.620	102.3	3.30	431409	0.53	9.65
0.40	5.771	101.3	3.43	441506	0.54	9.33
0.50	5.855	93.8	3.52	448443	0.54	9.11
0.60	5.922	85.0	3.60	453336	0.54	8.93
0.70	5.954	76.8	3.66	456482	0.54	8.79
0.80	5.961	69.0	3.71	457212	0.54	8.69
0.90	5.921	61.3	3.72	453394	0.54	8.65
1.00	-	-	-	-	-	-
	$k_p^{80°C}$ (m^3_{Pet}.mol-site^{-1}.s^{-1}) **1350**					
0.00	5.987	116.3	3.39	458938	0.52	9.26
0.10	6.115	114.0	3.50	468509	0.53	9.00
0.20	6.241	112.0	3.62	478461	0.53	8.76
0.30	6.370	110.3	3.74	489017	0.53	8.52
0.40	6.528	109.0	3.88	500509	0.54	8.24
0.50	6.640	101.5	3.99	509745	0.54	8.04
0.60	6.759	93.0	4.11	517857	0.54	7.82
0.70	6.845	85.0	4.21	525129	0.54	7.65
0.80	6.934	77.8	4.31	531551	0.54	7.47
0.90	6.978	70.5	4.39	535426	0.54	7.34
1.00	7.019	64.3	4.46	538299	0.54	7.21
	$k_p^{80°C}$ (m^3_{Pet}.mol-site^{-1}.s^{-1}) **1500**					
0.00	6.685	124.8	3.78	512309	0.52	8.29
0.10	6.827	122.3	3.91	523141	0.53	8.06
0.20	6.965	120.0	4.04	534385	0.53	7.85
0.30	7.126	118.3	4.18	546370	0.53	7.61
0.40	7.291	116.8	4.33	559274	0.54	7.38
0.50	7.457	109.5	4.48	570809	0.54	7.16
0.60	7.577	100.8	4.61	581568	0.54	6.98
0.70	7.743	93.3	4.76	592699	0.54	6.76
0.80	7.859	86.0	4.89	603368	0.54	6.59
0.90	6.389	79.5	5.04	613947	0.54	6.39
1.00	8.145	73.8	5.17	624621	0.54	6.21

3.4. Plot simulation results

The **simulation 1** fix total molar flow, **F**, inlet temperature, $\mathbf{T_0}$, and catalyst flowrate, $\mathbf{Q_c}$, for 3 different values of $\mathbf{k_p^{80°C}}$.

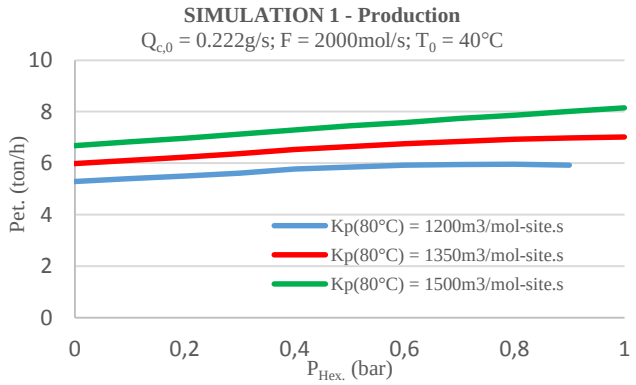

Figure 3 – Polyethylene mass rate steady-state simulations 1 results given the condition in plot title. Numerical output is in table 3.

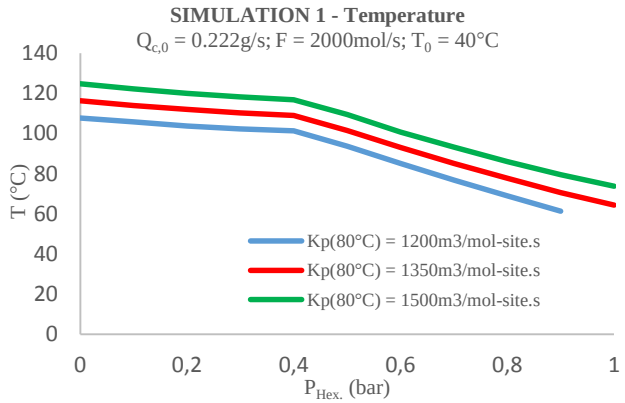

Figure 4 – Reactor temperature result simulation 1 given the conditions in plot title. Numerical data is in table 3

In the particularly set of conditions with $\mathbf{k_p^{80°C}=1200m^3_{Pet}mol\text{-}ac.^{-1}.s^{-1}}$ one can see there are no values for **1bar** hexane pressure. This is a particular case of thermodynamic constraint. The dew point of such inflow is above the reactor temperature. So there is no total vaporization making the gas-phase to have a different composition from the intended one.

The progress of curves in figure 3 show an increasing polyethylene rate production (about **2.5%** relative variation) with increasing hexane pressure/concentration in polymer phase. Moreover, curves appear to have a smaller relative variation in production as the hexane pressure increases, especially from starting of condensing mode. The 3 curves differ in propagation constant rate, $k_p^{80°C}$. Higher ones leads naturally to bigger production rates. The figure 4 shows a global decreasing temperature with increasing hexane pressure. From 0 to 0.4bar hexane pressure, the temperature gradually decreases (about **1.5%** relative variation) due to heat capacity of gases and after it, a more abrupt lowering of temperature (about **8%** relative variation) proceeds thanks to heat vaporization of condensed hexane (and ethylene). Polyethylene mass rate relative variation increases during dry-mode operation and then it starts to decrease. This is pronouncedly for set of $k_p^{80°C}$ = 1200 m^3mol-site$^{-1}s^{-1}$. As the hexane pressure increases, the liquid amount gets higher and the reactor temperature will drop due to considerable cooling capacity. At a certain value of hexane pressure, the reactor temperature gets too low and kinetics is clearly affected. For the other k_p's, since they are bigger, the related productions are more "slowly" affected.

For the 3 k_p's tested there are an average relative variation between them of about **15%** for polymer production. For temperature, there's a relative variation of about **10%** (in condensed-mode). It's also noticed a trend of decreasing of production and temperature relative variation between k_p's with increasing k_p. This is, in the k_p's presented, the biggest relative variations occurred between simulation sets of k_p's = 1200 m^3mol-site$^{-1}s^{-1}$ and k_p's = 1350 m^3mol-site$^{-1}s^{-1}$.

In the **simulation 2** (figures 5 and 6) there are 3 catalyst flow rates ($Q_{c.0}$) tested.

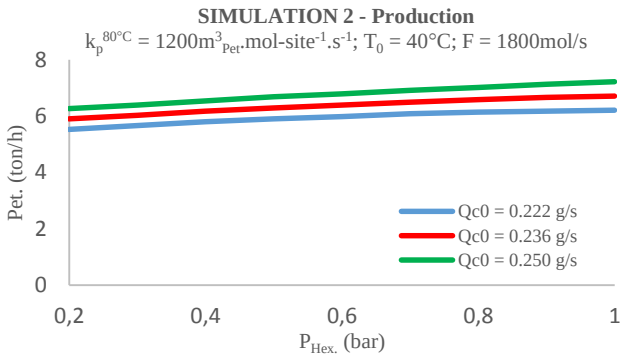

Figure 5 – Polyethylene mass rate steady-state simulations 2 results given the conditions in plot title.

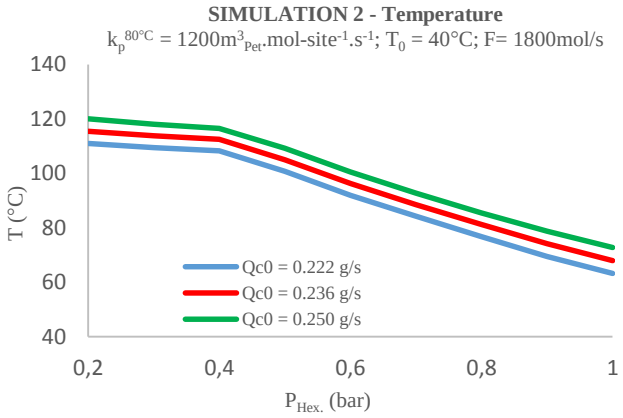

Figure 6 - Reactor temperature result simulation 2 given the conditions in plot title.

This simulation appears to have similar trends to the simulation 1. But here, because catalyst flowrates has not the same impact on temperature as kinetic constant, k_p, the highest relative variation between them is for production. For the three catalyst flow rates (Q_c) tested, there are a relative variation between them of about **9%** for polymer production and **7%** for temperature when reactor operates in condensed-mode. Since this relative variations are quite the same as the case of simulation 1, this may lead to the question of what preferably to boost: catalyst kinetic constant or catalyst flowrate for analogous productivity?! The cost factor might be the natural "decision variable". But in principle, catalyst kinetic constant in not immediately available to change unlike the catalyst flowrate. Temperature decreases with a smooth rate until 0.4bar hexane pressure and from this value on, it has a pronounced decreasing. For example, for $Q_{c.0}$ =

0.236g/s, from 0.2-0.4bar hexane pressure, the average rate of decreasing is about **1.5%** and from 0.5 bar on is about **8%**.

Simulation 3 results (figure 7 and 8) are lastly shown.

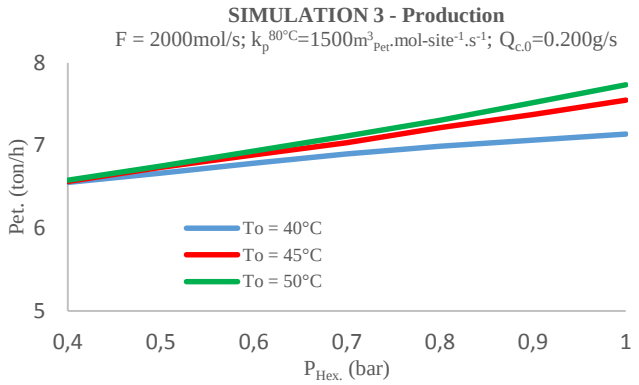

Figure 7 – Polyethylene mass rate steady-state simulations 3 results given the conditions in plot title

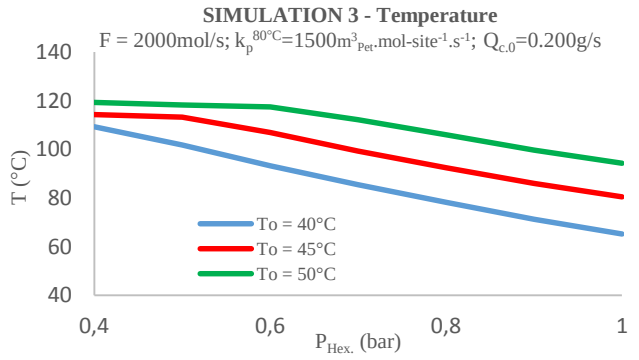

Figure 8 – Reactor temperature result simulation 3 given the conditions in plot title

Figure 7 shows there's small production difference especially between curves T_0 = 45°C and T_0 = 50°C. Actually before condensing mode (<0.5bar hexane), production is quite the same for 3 curves. Concerning case with T_0 = 40°C, it starts to deviate from the others at 0.5bar hexane (its condensed mode beginning). The production increases with hexane pressure, although moderately, and it seems to stabilize (and eventually even to decrease) near by the biggest hexane pressure tested (1.0bar). The other two curves start, in turn, to deviate from each other around 0.6bar hexane (starting cooling capacity for 45°C T_0 curve). Their individual progress show an increasing polyethylene rate production with increasing hexane concentration in polymer phase. For example, for T_0 = 45°C, the rate of polyethylene increasing is about 2.4% in average. Temperature decreases at a considerable rate with increasing hexane pressure. For example, for T_0 = 45°C, the average rate of decreasing is about 6%. They have pointedly more productivities with increasing hexane pressure when compared with 40°C T_0 case. This clearly remarks the cooling capacity influence in polymer production. 40°C T_0 curve will have a too high liquid content and it'll quickly make production to decrease. On the other side, for example 45°C T_0 curve has less liquid content and it will allow bigger productions not only due to higher temperatures but also because hexane pressure is higher and its co-solubility effect will be more active. For the three inlet flow temperatures there is very high temperature relative variation between them. For example at 0.8bar hexane, when inlet temperature changes from 45°C to 50°C, there is a temperature relative variation of about **15%**. And it is even higher between 40°C and 45°C (about 18%). These variations appear to decrease with increasing inlet temperature and increasing hexane pressure

This set of simulation indicates that differences in inlet temperature make substantial changes in production and reactor temperature. Basically, this happens because there's a big changing in flow composition in terms of liquid portion when the temperature changes, at least, 5°C (for instance, from 40 to 45°C). Even though hexane pressure gets higher – enhancing co-solubility effect and production in addition – if the liquid content in inlet flow is too high, it will soften the reaction.

3.5. Sensible analysis

The steady-state model simulated in this work naturally involves some physical quantities. And some of them may not be properly estimated for the work temperature and/or pressures. The sensible analysis will provide the information on equation balances terms that may have bigger deviations. Those ones should deserve more attention in the future for having better predictions and consequently allow accurate reactor simulations. The parameters were tested by varying its original simulation numerical value in a certain amount (percent) and observing the impact on the the polyethylene mass rate relative variation, Δm_{Pet} (%) and reactor temperature relative variation, ΔT (%). The parameters "perturbed" are those at **0.6bar hexane** and **0.9bar hexane** conditions, both related to **Simulation 1** results.

The sensible analysis for ethylene vaporization heat, $\mathbf{\Delta H_{v,et.}}$ and heat capacity of polymer phase, $\mathbf{C_{p,p}}$, **do not** have a relevant influence in model output. They were considerably perturbed in **200** and **100%** respectively varying **only -0.67%** and **-0.50%** in production for 0.6bar hexane condition. In opposite direction, solely **5%** ethylene concentration in polymer phase, $\mathbf{C_{et.}^{p}}$, perturbation leads to relative variation of **5.73% in production** and **3.82% in reactor temperature**. For example, a mere **5%** $\mathbf{C_{et.}^{p}}$ deviation would mean changing from **97.41mol/m^3_p** to **102.3mol/m^3_p**. It's just a small difference but it has a big impact in polyethylene production and in temperature as seen before. This emphasizes the importance of acquiring good predictions for this quantity.

Reaction enthalpy, $\mathbf{\Delta H_r}$, hexane equilibrium gas fraction in inlet stream, $\mathbf{y_{hex.}^{T0}}$ and hexane vaporization heat, $\mathbf{\Delta H_{v.hex.}}$, make reasonable changes in temperature. When they are, for the following order, perturbed in **+10**, **+15** and **+20%** they alter the reactor temperature in **6.50**, **5.00** and **-3.0°C**. With the largest difference in temperature from the original values comes gas heat capacity, $\mathbf{C_{p.g.}}$ deviation. When it varies **+20%**, the reactor temperature changes about **-8.3°C**. This may be explained with the fact the gas flowrate crossing the reactor is very big. There's in consequence a big amount of sensible heat and heat capacity becomes a sensible parameter in the context of this analysis

Conclusions

A gas-phase ethylene polymerization reactor working in condensed mode was simulated using a simple pseudo-homogeneous CSTR model. The main purpose was to

analyse the impact of n-hexane (ICA) in productivity and reactor temperature. The model included a simple approach composed by a single-site kinetics where the first-order ethylene concentration was predicted by Sanchez-Lacombe EOS. The particular aspect here was using an ethylene solubility Sanchez-Lacombe prediction for the ternary system – ethylene, n-hexane and polyethylene. This way the simulations for polymer production and reactor temperature were taking into account the co-solubility effect of n-hexane.

A global evaluation of simulations indicates an increasing of about **2%** of production as the n-hexane pressure increases **0.1bar** while there's no too much cooling capacity able to ease kinetics. With respect to temperature, there's a significant decreasing of about **8%** when the reactor is operating in condensed-mode in contrast with only **1.5%** when it is operating in a dry regime. At some point of inlet liquid content – associated with higher hexane pressures – the heat removal makes the reaction temperature to fall down too much and kinetics is diminished.

The simulations tested different **kinetic constants** ($\mathbf{k_p}$), different **catalyst flowrates** and different **inlet gas temperatures**. The changing of kinetic constants led to a relative variation between them of **15%** for production and **10%** for temperature. Changing the catalyst flowrate meant a relative variation of **9%** for production and **7%** for temperature. On the other way, when the **inlet stream temperature** is changed, the polymer production is differently trended: for the lowest inlet stream temperature, production grows less and decreases faster. The other two inlet temperatures tested seem to be more production maximized given the operation conditions.

From the sensitive analysis, the main parameters causing bigger deviations are hexane vaporization heat - influencing productivity and temperature, gas heat capacity – influencing productivity and temperature, vapour composition of inlet flow gas – influencing temperature, as well as polymerization heat influencing a lot temperature. The concentration of ethylene in polymer phase have a pronounced impact on production and temperature.

It would be interesting to simulate the model with other alkanes with different heat capacities and co-solubility effects than from those of n-hexane, namely isopentane and n-butane. In addition, for similar co-solubility and heat removal behaviour, economic and n-alkane easier degasing operation from polymer particles may also be a factor for ICA's choosing. As it was referred, n-hexane has a very high solubility in polyethylene compared with other similar n-alkanes. This will promote the co-solubility effect (positive) but it also intensifies the degasing operation of polymer particles (negative).

The reactor simulations in this thesis are based on a very simple reactor model. Continuing the current work will mean adopting more realistic reactor models, in a dynamic approach, where they can combine not only mature polymerization times but also initial ones (with related kinetics). Catalyst size distribution as well as catalyst residence time should incorporate such models since industrial catalyst particles are not all uniform in their size and they remain different times in the reactor. This factors affect kinetics and productivity/temperature by extension. Howsoever the results obtained here were suitable for reproducing the effect of the ICA n-hexane in PE productivity and temperature and they may be also a comparison basis for other works in this field.

References

[1] Sanchez, I. C., Lacombe, R. H. (1978), Statistical thermodynamics of Polymer solutions, *Macromolecules, 11*, 1145-1156

[2] Guerrieri, Y., Pontes, K., V., Costa, G., M., N., Embiruçu, M. (2011); A survey of equations of state for polymers, Industrial engineering program - Universidade federal da Bahia, Salvador-BA, Brazil.

[3] J. Kosek, Z. Grof, A. Novák, F. Stepánek, M. Marek (2001), Dynamics of particle growth and overheating in gas-phase polymerization reactors, *Chemical Engineering Science, 56*, 3951-3977

[4] Kunni D., Levenspiel O. (1991), Fluidization Engineering, 2nd ed., Butterworth Heinemann, London.

[5] S. Floyd, K.Y. Choi, T.W. Taylor, W.H. Ray (1986), Polymerization of olefins through heterogeneous catalysts. Polymer particle modelling with an analysis of intraparticle heat and mass transfer effects, *Journal of Applied Polymer Science, 32*, 2935-2960.

[6] Ray, W., & Hutchinson, R. (1990), Polymerization of olefins through heterogeneous catalysis. VIII. Monomer sorption effects, *Journal of Applied Polymer Science, 41*, 51-81.

[7] Yao, W.; Hu, X.; Y., Yang, Y., (2007), Modeling the Solubility of Ternary Mixtures of Ethylene, iso-Pentane,n-Hexane in Semicrystalline Polyethylene, *Journal of Applied Polymer Science, 103*, 3654-3662.

[8] Bashir, A. M.; Ali, M. A.; Kanellopoulos, V.; Seppälä, J., (2013), Modelling of multicomponent olefins solubility in polyolefins using Sanchez–Lacombe equation of state, *Fluid Phase Equilibria, 358*, 83-90.

[9] Alizadeh, A., (2014), Study of sorption, heat and mass transfer during condensed-mode operation of gas phase ethylene polymerization on suported catalyst, Kingston, Canada.

[10] Wagner, B. E., Goeke, G. L., Karol, F.J. (1981), US. Patent 4.303.771, United States.

[11] McAuley, K.B., Talbot, J.P., Harris, T.J. (1994), A comparison of two-phase and well-mixed models for fluidized bed polyethylene reactors, *Chemical Engineering Science, 49*, 2035-2045.

[12] Xie, T., McAuley, K. B., Hsu, J. C. C., & Bacon, D. W. (1994), Gas phase ethylene polymerization: Production processes, polymer properties and reactor modelling, *Ind. Eng. Chem. Res., 33*, 449-479.

[13] Wu, S.Y., Baeyens, J. (1998), Segregation by size difference in gas fluidized beds, *Powder Technology, 98*, 139-150.

[14] Choi, K. Y.; Ray, W. H. (1985), The dynamic behaviour of fluidized bed reactors for solid catalyzed gas phase olefin polymerization, *Chemical Engineering Science, 40*, 2261-2279.

[15] Lynch, D. T.; Wanke, S. E. (1991), Reactor design and operation for gas-phase ethylene polymerization using Ziegler-Natta catalyst, *Canadian Journal of Chemical Engineering, 69*, 332-339.

[16] Alizadeh, M., Mostoufi, N., Pourmahdian, S., Sotudeh-Gharebagh, R. (2004), Modeling of fluidized bed reactor of ethylene polymerization, *Chemical Engineering Journal, 97*, 27-35.

[17] Weijuan, M., Jianwei, L., Hongbo, L. (2013), Modeling and Simulation of Ethylene Polymerization in Industrial Slurry Reactor Series, *Chinese Journal of Chemical Engineering, 21*, 850-859.

[18] Banat, Yahya; Al-Obaidi, Fahad; Malek, Abdul Kader (2014), US Patent 8.669.334 B2, *Saudi Basic Industries Corporation, Riyadh (SA)*, United States.

[19] Ramanathan, Ashuraj Sirohi & Sundaram (1998), Design Issues in Converting to Super-Condensed Mode Operation for Polyethylene (1-7), *AIChE Spring 98 Meeting*, New Orleans.

[20] Mirzaei, A.; Kiashemshaki, A.; Emani, M.; (2007), Fluidized Bed Polyethylene Reactor Modeling in Condensed Mode Operation, *Macromol. Symp., 259*, 135-144.

[21] A. Alizadeh, Timothy F. L. McKenna, (2013), Condensed Mode Cooling in Ethylene Polymerization: droplet evaporation, *Macromol. Symp., 333*, 242-247.

[22] NIST, National Institute of standards and technology (08/10/2014), http://webbook.nist.gov/cgi/cbook.cgi?ID=C110543&Mask=4.

[23] Smulaka, J., Span, R., Wagner, W. (2001), New equation of state for ethylene covering the fluid region for temperatures from the melting line to 450K at pressures up to 300Mpa, *AIP publishing*, 1057-1097.

[24] Jenkins J.M., Jones R.L., Jones T.M. (1986), Patent US 4.588.790 – Method for fluidized bed polymerization, Danbury, USA.

[25] Griffin et al. (1995), Patent US 5.462.999 - Process for polymerizing monomers in fluidized beds, Wilmington, USA.